NASA TECHNICAL NOTE

NASA TN D-7727

NASA TN D-7727

SOME ASPECTS OF OPTICAL FEEDBACK WITH CADMIUM SULFIDE AND RELATED PHOTOCONDUCTORS

by Stephen J. Katzberg

Langley Research Center
Hampton, Va. 23665

NATIONAL AERONAUTICS AND SPACE ADMINISTRATION • WASHINGTON, D. C. • NOVEMBER 1974

1. Report No.	2. Government Accession No.	3. Recipient's Catalog No.
NASA TN D-7727		

4. Title and Subtitle	5. Report Date
SOME ASPECTS OF OPTICAL FEEDBACK WITH CADMIUM SULFIDE AND RELATED PHOTOCONDUCTORS	November 1974
	6. Performing Organization Code

7. Author(s)	8. Performing Organization Report No.
Stephen J. Katzberg	L-9634
	10. Work Unit No. 502-03-52-04
9. Performing Organization Name and Address	11. Contract or Grant No.
NASA Langley Research Center Hampton, Va. 23665	
	13. Type of Report and Period Covered
12. Sponsoring Agency Name and Address	Technical Note
National Aeronautics and Space Administration Washington, D.C. 20546	14. Sponsoring Agency Code

15. Supplementary Notes

16. Abstract

A primary limitation of many solid-state photoconductors used in electro-optical systems is their slow response in converting varying light intensities into electrical signals. An optical feedback technique is presented which can extend the frequency response of systems that use these detectors by orders of magnitude without adversely affecting overall signal-to-noise ratio performance. The technique is analyzed to predict the improvement possible and a system is implemented using cadmium sulfide to demonstrate the effectiveness of the technique and the validity of the analysis.

17. Key Words (Suggested by Author(s))	18. Distribution Statement
Optical detection Photoconductor Optical feedback	Unclassified – Unlimited STAR Category 14

19. Security Classif. (of this report)	20. Security Classif. (of this page)	21. No. of Pages	22. Price*
Unclassified	Unclassified	36	$3.25

*For sale by the National Technical Information Service, Springfield, Virginia 22151

SOME ASPECTS OF OPTICAL FEEDBACK WITH CADMIUM SULFIDE AND RELATED PHOTOCONDUCTORS

By Stephen J. Katzberg
Langley Research Center

SUMMARY

A primary limitation of many solid-state photoconductors used in electro-optical systems is their slow response in converting varying light intensities into electrical signals. An optical feedback technique is presented which can extend the frequency response of systems that use these detectors by orders of magnitude without adversely affecting overall signal-to-noise ratio performance. The technique is analyzed to predict the improvement possible and a system is implemented using cadmium sulfide to domonstrate the effectiveness of the technique and the validity of the analysis.

INTRODUCTION

The applicability of many solid-state photoconductors to electro-optical systems is limited not only by the inherent slow response of many of them but also by the variation of response time with ambient illumination. Simple frequency compensation to recover the response time attenuated signal can be a fruitless task. This is unfortunate because, in many cases, the actual signal-to-noise ratio available from the photoconductor is constant into the kilohertz range (see, for example, ref. 1) even though the photoconductor internal 3 dB frequency may only be of the order of 1 Hz.

Optical feedback can be used to improve the frequency response of these detectors by introducing a biased, negative feedback light signal so that the photodetector is stimulated by both the signal radiation and the feedback signal (ref. 2). The use of negative feedback allows a trade-off between signal gain and signal bandwidth. Furthermore, as long as the dominant noise in the system is that from the photoconductor, basic signal-to-noise ratios are unaffected.

There is further improvement when optical feedback is applied to photoconductors such as cadmium sulfide (CdS) which have ambient light dependent response times. Since optical feedback works to maintain a constant illumination on the photoconductor, the response time becomes signal independent and adjustable.

The purpose of this paper is to present some aspects of the application of optical feedback to cadmium sulfide and similar slow response time optical detectors. A review of the characteristics of photoconductors is presented, especially of those points that have a bearing on the use of cadmium sulfide with optical feedback. The optical feedback technique is analyzed with general considerations as to its effect on signal-to-noise ratio. Some ideas as to maximum amount of frequency response extension and overall system dynamic stability are given. The characteristics of cadmium sulfide are incorporated into the analysis to provide a concrete example. Finally, results are presented of an experimental realization of a CdS optical feedback system that demonstrates the validity of the analysis.

SYMBOLS

$\mathcal{A}$	area, centimeters^2
A	amplifier gain, volts/ampere
A_L	system loop gain
ΔB	bandwidth interval, hertz
C	amplitude constant for 1/f noise, centimeter^3-hertz
D*	detectivity, centimeter-hertz$^{1/2}$/watt
e	electronic charge, 1.6×10^{-19} coulomb
F	intensity of excitation, absorbed photons/second-centimeter^3
f	frequency, hertz
f_M	frequency above which system detectivity degrades, hertz
f_T	operational amplifier unity gain frequency, hertz
G	photoconductor gain
G_f	conductance of system feedback resistor, siemens

G_λ	wavelength dependent photoconductor conductance, siemens
G'_λ	renormalized wavelength dependent photoconductor conductance, siemens
$G_{\lambda,0}$	dark conductance of photoconductor, siemens
h	Planck's constant, 6.626×10^{-34} joule-second
I	current, amperes
I_{dc}	zero frequency component of current, amperes
I_{gr}	generation-recombination noise current, amperes/$\sqrt{\text{hertz}}$
I_{JN}	rms Johnson noise current, amperes/$\sqrt{\text{hertz}}$
$I_{N,A}$	operational amplifier rms noise current, amperes/$\sqrt{\text{hertz}}$
$I_{N,t}$	total rms noise current of photoconductor, amperes/$\sqrt{\text{hertz}}$
$I_{1/f}$	rms value of 1/f noise current, amperes/$\sqrt{\text{hertz}}$
K	first order frequency dependent photoconductor sensitivity factor, siemens/watt
K'	second order frequency dependent photoconductor sensitivity factor, siemens/watt^2
K_0	zero frequency value of first order frequency dependent photoconductor sensitivity factor, siemens/watt
K'_0	zero frequency value of second order frequency dependent photoconductor sensitivity factor, siemens/watt^2
k	system loop gain at zero frequency
k	Boltzmann's constant, 1.38×10^{-23} joule/kelvin
l	linear dimension, centimeters

N	total of free carriers
n	density of free carriers, number/centimeter^3
n_t	density of trapped carriers, number/centimeter^3
P	power in a photon stream with rate Φ, watts
P_e	effective bias radiant power, watts
P_f	optical feedback power, watts
P_i	video radiant power, watts
P_N	rms noise power in a photon stream with rate Φ, watts
R_B	amplifier bias resistance, ohms
R_D	diode series resistance, ohms
R_f	feedback resistance, ohms
R_λ	photoconductor resistance (= $1/G_\lambda$), ohms
S	photoconductor sensitivity, siemens-centimeter^2/watt
S_D	feedback-light coupling factor, watts/ampere
s	Laplacian operator
T	absolute temperature, kelvins
V	supply voltage, volts
V_B	amplifier offset bias, volts
$V_{N,S}$	total system noise voltage, volts/hertz$^{1/2}$
$V_{N,1}$	rms noise voltage of photoconductor, volts/hertz$^{1/2}$

$V_{N,2}$	rms noise voltage of operational amplifier, volts/hertz$^{1/2}$
$V_{N,3}$	Johnson noise voltage of feedback resistor, volts/hertz$^{1/2}$
$V_{N,4}$	Johnson noise voltage of bias resistor, volts/hertz$^{1/2}$
V_o	output signal, volts
V_s	detector bias, volts
α	normalized relative spectral sensitivity of photoconductor
Δ	denotes change in a variable
μ	carrier mobility, centimeters^2/volt-second
ν	frequency of light radiation, hertz
ρ	dynamic range
σ	conductivity, siemens/centimeter
τ	free carrier lifetime in photoconductor, seconds
τ_o	observed internal response time of photoconductor, seconds
τ_1	first operational amplifier time constant, seconds
τ_2	second operational amplifier time constant, seconds
Φ	photon arrival rate, photons/second
Φ_N	rms noise in a photon particle stream, photons/second

PHOTOCONDUCTOR CHARACTERISTICS

To properly analyze the use of photoconductors in the optical feedback configuration, it is necessary to review the models of photoconductor electrical characteristics. They

are presented in four parts: simple photoconductivity, response time, figures of merit, and noise. Particular emphasis is placed on cadmium sulfide because of its extremely high sensitivity and its wide availability. Much of the information presented herein is abstracted from reference 3 and the interested reader is referred there and to reference 4 for more discussion.

Photoconductivity

The basic conductivity of a solid is described by the relation

$$\sigma = ne\mu \tag{1}$$

where n is the density of free carriers, e is the electronic charge, and μ is the carrier mobility. It has been assumed that the only n-type carriers are present. The change in conductivity under the influence of an excitation F that generates $n = F\tau$ carriers (where τ is the free carrier lifetime) is

$$\Delta\sigma = e\mu\Delta(F\tau) + ne\Delta\mu = e\mu\tau\Delta F + e\mu F\Delta\tau + ne\Delta\mu \tag{2}$$

where ΔF, $\Delta\tau$, and $\Delta\mu$ are the changes in these variables from their steady-state values. For simplicity, it will be assumed that the changes in μ and τ are of much less effect than the change in n, or

$$\Delta\sigma \approx e\mu\tau\Delta F \tag{3}$$

This equation states that to first order the conductivity change varies linearly with change in excitation.

Speed of Response

The observed speed of response for photoconductors is often much lower than that which would correspond to the free carrier lifetime. The reason for the slow response is that photosensitive CdS contains various types of trapping centers so that when light is applied to a photoconductor, the photoexcited electrons divide into two components: one supplies the free carriers and the other feeds the traps. At low light levels the latter is the primary destination of the electrons until the traps are sufficiently filled, after which the free carrier density increases. The converse is true for the period after photoexcitation has ceased. Trapped electrons continue to be released until a new steady state is reached. According to reference 3 the observed decay time can be correlated approximately with the free carrier lifetime by the relation

$$\tau_o = \frac{\tau n_t}{n} \tag{4}$$

where τ_o is the observed decay time, τ is the free carrier lifetime, and n_t is the density of trapped carriers within about kT of the steady-state Fermi level. The equation only holds for $\tau_o \geqq \tau$. Note that equation (4) indicates a strong dependence of the lifetime on ambient conditions.

Figures of Merit

In order to compare various photoconductive cells and materials, it is useful to introduce two figures of merit. The first is photoconductor specific sensitivity, basically a material parameter. The second is photoconductor gain, a cell parameter.

The photoconductor specific sensitivity S is defined by the following relation:

$$S = \frac{(\Delta I/V)l^2}{P} \tag{5}$$

where ΔI is the photocurrent, V is the applied voltage, l is the electrode spacing, and P is the absorbed radiation power. Sensitive CdS has values of S in the range from 0.1 to 1.0 cm^2/Ω-W. Note that S is independent of geometry, applied field, and applied light intensity (ref. 4).

By noting that the conductance of a rectangular slab of photoconductor is

$$\frac{\Delta I}{V} \equiv R_\lambda^{-1} = \frac{e\mu\mathcal{A}\Delta n}{l} \tag{6}$$

where l is the electrode separation and $\mathcal{A}$ is the area of the electrodes, S can be written

$$S = \frac{e\mu\mathcal{A}l\Delta n}{P} = \frac{e\mu\Delta N}{P} \tag{7}$$

where ΔN is the free carrier density Δn multiplied by the volume of the sample. Using the relation $\Delta n \approx \tau\Delta F$ and noting that $P \propto \Delta F$ results in

$$S \propto \mu\tau \tag{8}$$

Note that, at constant μ, the longer the response time the higher the sensitivity becomes, as was stated earlier.

The gain G of a photoconductor is defined as the number of carriers that pass between the electrodes (with separation l) for each photon absorbed. Since the velocity of a free carrier is $V\mu/l$, G may be expressed as

$$G = \frac{V\mu\tau}{l^2} \tag{9}$$

It can be seen that G is proportional to the photoconductor specific sensitivity S through its dependence on μ and τ. For CdS, typical values of G are in excess of 10^4.

Noise

The usefulness of CdS results from its high detectivity which, in turn, results from the fact that the detector is nearly photon noise limited (see ref. 5). The high detectivity of a photoconductor such as CdS would be of little use in ac photodetection, however, if its internal noise and signal output have the same frequency dependence. To examine the useful range for ac operation of photoconductors, it is necessary to consider the noise processes occurring in photoconductors. Normally, three noise sources are associated with any photoconductor: Johnson or resistor noise, generation-recombination (g-r) noise, and contact or 1/f noise (ref. 6).

Johnson noise represents the result of random motion of existing free carriers and will contribute an amount of squared noise current per Hz to an external circuit expressed by the following equation:

$$I_{JN}^2 = \frac{4kT}{R_\lambda} \tag{10}$$

where k is Boltzmann's constant, T is absolute temperature, and R_λ is device resistance.

The second squared noise component (that is, g-r noise) results from the random removal from the conduction process of free carriers either by trapping or recombination. This g-r noise component is shown in reference 4 or reference 7 to be of the form (per Hz)

$$I_{gr}^2 = \frac{4eI_{dc}G}{1 + (2\pi f\tau_o)^2} \tag{11}$$

where I_{dc} is the steady-state device current. In general, g-r noise dominates or can be made to dominate the noise in a photoconductor. Note that its frequency dependence is that of the signal.

The last noise source of interest is 1/f or contact noise. This noise can be reduced, if not eliminated, by good contacts (ref. 5) and takes the form (per Hz)

$$I_{1/f}^2 = \frac{CI_{dc}^2}{\mathcal{A} f l} \tag{12}$$

where C is a constant which is evaluated empirically.

Following reference 6 it is possible to assemble these noise sources and to write for the overall squared noise current per unit bandwidth in a photoconductor:

$$I_{N,t}^2 = \frac{4kT}{R_\lambda} + \frac{4eGI_{dc}}{1 + (2\pi f \tau_o)^2} + \frac{CI_{dc}^2}{\mathcal{A} f l} \tag{13}$$

Note that the second term, the g-r noise varies as I_{dc}^2 since from equation (9) G varies with V in the same way that I_{dc} does. It is also clear that the g-r noise (and 1/f noise) can be made to dominate the purely resistive noise. However, there will be a frequency at which the frequency dependent noises will reduce to the flat Johnson noise component. Above this frequency the signal-to-noise ratio will begin to degrade. Consequently, this frequency represents the highest frequency at which the maximum photoconductor detectivity can be realized. If, for a moment, the 1/f component is ignored in order to determine an upper bound, this frequency of equality is

$$f_M \approx \frac{1}{2\pi} \frac{1}{\tau_o} \left(\frac{eGV}{kT}\right)^{1/2} \tag{14}$$

or, for the typical CdS values of $G \geqq 10^4$, $V \approx 10$ volts, and room temperature operation,

$$f_M \geqq \frac{2 \times 10^3}{2\pi\tau_o} \tag{15}$$

Experimental results (see, for example, ref. 1) have shown that, for internal response frequencies of about 0.1 Hz, the CdS signal-to-noise ratio could be constant up to 10 kHz, which is in reasonable agreement with equation (15).

OPTICAL FEEDBACK ANALYSIS

To understand the optical feedback technique when applied to photoconductors, it is necessary to apply the ideas of the previous section in conjunction with the ideas of negative feedback analysis. Therefore, the basic analysis of an optical feedback with noise

sources is considered. The dynamic stability and validity of the frequency extension idea are analyzed to determine the limits of possible frequency extension. Finally, the trade-off between frequency response and dynamic range is presented, because it is particularly important in photon noise limited photoconductors.

Basic Analysis

A circuit that utilizes the optical feedback technique is shown in figure 1. This circuit consists basically of a high-gain light-to-voltage converter with the frequency limited nonlinear photoconductor (in this case CdS) inside the feedback loop. The feedback element in this case is a visible light-emitting diode (LED) whose light-out versus current-in characteristic is linear over several decades.

The relations governing the basic operation of this system are now described. The following equation describes the output of the operational amplifier (see ref. 8):

$$-V_o(s) = V_s R_f G_\lambda(s) + V_B \frac{R_f}{R_B} \tag{16}$$

where G_λ is the conductance of the photodetector, and the other quantities are as shown in figure 1.

The next step is to introduce an artifice into this equation which eliminates the dark conductance of the photoconductor; that is,

$$-V_o = V_s R_f G_{\lambda,0} + V_s R_f (G_\lambda - G_{\lambda,0}) + V_B \frac{R_f}{R_B} \tag{17}$$

The difference $G_\lambda - G_{\lambda,0}$ is only a function of the light on the photoconductor and is zero for zero light. This difference can be rewritten as the functional relationship

$$G_\lambda - G_{\lambda,0} = G'_\lambda(\alpha P_i, P_f) \tag{18}$$

to demonstrate the effect of the two light sources: input and feedback. Although G'_λ may be nonlinear, it is assumed to be monotonic. The factor α is the normalized relative spectral responsivity of the photodetector or, more precisely, the relative response of the photodetector to the incident light P_i as compared with its response to the feedback light P_f from the light-emitting diode.

The effect of the light-emitting diode may be included in the form

$$P_f = \frac{S_D}{R_D} V_o \tag{19}$$

where S_D is a coefficient which accounts for the radiant power (in watts) incident on the photodetector as a function of LED current (in amperes) and includes, therefore, the geometry between diode and photodetector. Substituting equation (19) into equation (18) and combining with equation (17) yields

$$-V_o = V_s R_f G_{\lambda,0} + V_s R_f G'_\lambda\left(\alpha P_i, \frac{S_D}{R_D} V_o\right) + V_B \frac{R_f}{R_B} \tag{20}$$

Equation (20) may be linearized around the operating point to take a form more like a standard feedback system; that is,

$$-V_o \approx V_s R_f G_{\lambda,0} + V_s R_f K \Delta P + V_B \frac{R_f}{R_B} \tag{21}$$

where $\Delta P = \alpha P_i + \frac{S_D}{R_D} V_o$, and K is defined in the Taylor series expansion:

$$G'_\lambda \approx \frac{dG'_\lambda}{dP} \Delta P + \frac{1}{2} \frac{d^2 G'_\lambda}{dP^2} (\Delta P)^2 + \ldots = K\Delta P + K'(\Delta P)^2 + \ldots \tag{22}$$

The parameter K can be identified as S/l^2 by referring to equations (22) and (5). Both K and K' carry the frequency dependence of the photoconductor, with K_0 and K'_0 the zero frequency values appropriate to each. Rewriting equation (21) with a little manipulation gives as a first order approximation

$$V_o = \frac{V_s R_f G_{\lambda,0} + V_B \frac{R_f}{R_B}}{1 + V_s R_f K_0 \frac{S_D}{R_D}} - \frac{V_s R_f K \alpha P_i}{1 + V_s R_f K \frac{S_D}{R_D}} \tag{23a}$$

If the loop gain $A_L = V_s R_f K \frac{S_D}{R_D}$ is much greater than unity, equation (23a) reduces to

$$V_o = -\frac{1}{R_f V_s}\left(V_s R_f G_{\lambda,0} + V_B \frac{R_f}{R_B}\right)\frac{R_D}{K_0 S_D} - \frac{R_D}{S_D} \alpha P_i \tag{23b}$$

or more conveniently

$$V_o = -\frac{R_D}{S_D} \alpha P_i - \frac{R_D}{S_D} P_e \tag{23c}$$

where

$$P_e = \frac{1}{K_0 R_f V_s}\left(V_s R_f G_{\lambda,0} + V_B \frac{R_f}{R_B}\right)$$

The formulation given by equation (23c) reveals two important aspects of the optical feedback concept:

(1) The output voltage depends on the constant term P_e, which can be removed, and on P_i, the incident absorbed power. For loop gains much larger than unity, the input-output frequency response to light will be determined by the feedback diode frequency response (which is generally flat to several MHz). As the loop gain approaches unity, the input-output response will again be dominated by the photodetector frequency response. Stated another way, the product of system gain and bandwidth for a high loop gain is constant. Practical increases in frequency response are discussed in more detail later.

(2) For loop gain much greater than unity, the output voltage V_O is linear with respect to the input power P_i. This result is also found to be true in a more detailed analysis and represents the familiar linearizing effect of feedback. Although important, this effect is not as critical as poor frequency response in the detection of low light levels and is not pursued further here.

Effect of Noise Sources

In order to study the response of the optical feedback system to noise, it is necessary to modify equation (16) to include the noise sources shown in figure 2, which results in the following equation:

$$-V_o = V_s R_f G_\lambda + V_B \frac{R_f}{R_B} + \left[\left(V_{N,1} G_\lambda R_f\right)^2 + \left(V_{N,4} \frac{R_f}{R_B}\right)^2 + \left(V_{N,3}\right)^2 + \left(V_{N,2}\right)^2 \left(G_\lambda R_f + \frac{R_f}{R_B} + 1\right)^2 + \left(I_{N,A} R_f\right)^2\right]^{1/2} \tag{24}$$

where each noise component in the bracketed quantity is summed in the root-sum-of-squares (rss) sense.

By continuing the analysis as before, the following equation is easily obtained:

$$V_o = -\frac{V_s R_f G_{\lambda,0} + V_B \frac{R_f}{R_B}}{1 + V_s R_f K \frac{S_D}{R_D}} - \frac{V_s R_f K \alpha P_i}{1 + V_s R_f K \frac{S_D}{R_D}}$$

$$+ \left[\frac{\left(V_{N,1} G_\lambda R_f\right)^2 + \left(V_{N,4} \frac{R_f}{R_B}\right)^2 + \left(V_{N,3}\right)^2 + \left(V_{N,2}\right)^2 \left(G_\lambda R_f + \frac{R_f}{R_B} + 1\right)^2 + \left(I_{N,A} R_f\right)^2}{\left(1 + V_s R_f K \frac{S_D}{R_D}\right)^2} \right]^{1/2} \tag{25}$$

where again the bracketed quantity is an rss sum. Note that the denominator of equation (25) is affected at least by the frequency dependence of K. Thus, the noise component of equation (25) is reduced by the dc value of loop gain at sufficiently low frequency.

Examination of the signal component of equation (25) shows that it is similarly affected by the loop gain. Thus, in the case where the noise has a similar frequency dependence as K, the signal-to-noise ratio will remain constant and equal to the nonfeedback case. As described earlier, the signal-to-noise ratio will continue to be constant until the noise reaches a region of frequency dependence that does not decrease as rapidly with frequency as does the signal.

To examine these analytical results in more detail, consider the nature (or assumed nature) of the various noise components in equation (24).

The noise source $V_{N,1}$ represents the noise generated by the photoconductor. Generality will be retained here, since several photoconductors tend to show similar dependence of their noise on the same parameters (refs. 4 and 6). Thus, by using the value for the noise current per $Hz^{1/2}$ given in equation (13), the noise voltage per $Hz^{1/2}$ of the photoconductor is

$$V_{N,1} = R_\lambda I_{N,t} = R_\lambda \left[\frac{4kT}{R_\lambda} + \frac{4eGI_{dc}}{1 + (2\pi f \tau_o)^2} + \frac{CI_{dc}^2}{\mathcal{A} f l} \right]^{1/2} \tag{26}$$

Note that at low frequencies the last term dominates and at high frequencies the first term dominates. The exact balance among the three quantities depends on the type of photoconductor, as discussed later.

The noise source $V_{N,2}$ is the noise voltage associated with the operational amplifier which commonly has both a small 1/f characteristic as well as a flat spectrum. For a complete discussion of noise sources in operational amplifiers the reader is referred to reference 8. Since the primary effect of the amplifier noise voltage is to limit the high frequency signal-to-noise ratio, this noise voltage is assumed to be flat.

The third noise source $V_{N,3}$ is that associated with the feedback resistance R_f and has a value $\left(\text{per } \text{Hz}^{1/2}\right)$ expressed as

$$V_{N,3} = (4kTR_f)^{1/2} \tag{27}$$

Note that this noise voltage is flat with frequency.

Similarly, $V_{N,4}$ is the noise voltage associated with the bias resistor, is flat with frequency, and, per $\text{Hz}^{1/2}$, is given by

$$V_{N,4} = (4kTR_B)^{1/2} \tag{28}$$

The last noise source to be considered is the so-called "open circuit" current noise (ref. 8) of the operational amplifier $I_{N,A}$. This noise source is indicated in figure 2 and for the frequencies of interest herein will be small compared to the resulting noise from the other sources.

It is now possible to assemble the various modeled noise sources to give the total output noise voltage in equation (25) as

$$V_{N,S}^2 = R_f^2 \left\{ 4kT\left(G_\lambda + \frac{1}{R_B} + G_f\right) + V_{N,2}^2\left(G_\lambda + \frac{1}{R_B} + G_f\right)^2 + \frac{4eGV_s}{R_\lambda\left[1 + (2\pi f\tau_o)^2\right]} + CV_s^2 \frac{G_\lambda^2}{\mathcal{A}fl} \right\} \left(\frac{1}{1 + KV_sR_f \dfrac{S_D}{R_D}} \right)^2 \tag{29}$$

Note that the loop gain is

$$A_L = V_sR_fK\frac{S_D}{R_D}$$

Substituting $K = \frac{dG'_\lambda}{dP} = \frac{S}{l^2}$, and with P given in watts, results in

$$A_L = V_S R_f \frac{S}{l^2} \frac{S_D}{R_D} \tag{30}$$

The desired output signal

$$V_o = \frac{V_S R_f K \alpha P_i}{1 + V_S R_f K \frac{S_D}{R_D}} \tag{31}$$

divided by the noise gives the rms signal-to-noise ratio

$$\frac{S}{N} = \frac{V_S K \alpha P_i}{\left\{ 4kT\left(\frac{1}{R_\lambda} + \frac{1}{R_B} + \frac{1}{R_f}\right) + V_{N,2}^2 \left(\frac{1}{R_\lambda} + \frac{1}{R_B} + \frac{1}{R_f}\right)^2 + \frac{4eGV_S}{R_\lambda\left[1 + (2\pi f \tau_o)^2\right]} + \left(\frac{V_S}{R_\lambda}\right)^2 \frac{C}{\mathcal{A} f l} \right\}^{1/2}} \tag{32}$$

or, if $R_\lambda \ll R_B$ and $R_\lambda \ll R_f$,

$$\frac{S}{N} = \frac{V_o}{V_{N,S}} = \frac{V_S K \alpha P_i}{\left\{ 4kTG_\lambda + V_{N,2}^2 G_\lambda^2 + \frac{4eGV_S}{R_\lambda\left[1 + (2\pi f \tau_o)^2\right]} \right\}^{1/2}} \tag{33}$$

assuming for the moment that $C \approx 0$, that is, assuming that the 1/f noise component can be made negligible (see ref. 5) to yield conditions for maximum performance.

It was postulated earlier that the frequency response of K was that of the photoconductor. Furthermore, as noted earlier, if the photoconductor noise dominates the other noise mechanisms, then there will again be a range of frequencies in which the signal-to-noise ratio will be constant. However, the new maximum frequency for undegraded detectivity will be reduced under the influence of the additional system noise sources.

The new maximum frequency of undegraded noise performance can be found from the denominator of equation (33) by setting the frequency dependent components of the noise equal to the flat noise components to give

$$\frac{4eGV_S}{R_\lambda\left[1 + (2\pi f_M \tau_O)^2\right]} = \frac{4kT}{R_\lambda} + \frac{V_{N,2}^2}{R_\lambda^2} \tag{34}$$

Solving for f_M yields

$$f_M = \frac{1}{2\pi\tau_O}\left(\frac{4eGV_S R_\lambda}{4kTR_\lambda + V_{N,2}^2}\right)^{1/2} \tag{35}$$

This new maximum frequency is similar to that in equation (15) but includes the effect of the operational amplifier on noise performance.

Dynamic Stability and Frequency Response

There is a limit to the amount of optical feedback which can be applied without instability. Presented here are some simple considerations that allow an idea of this limit. The problem is approached from the point of view of a first order analysis directed towards obtaining the maximum frequency response possible without overshoot and ringing.

Ideal case.- The analysis presented so far has indicated that only the photoconductor time constant is present in the optical feedback system. Thus, the system impulse response would be that of a single pole system and should cause a simple low pass filtering effect. However, it is easy to see that the operational amplifier and LED should also have certain time constants which affect system frequency response.

The ideal situation can be established as follows: Let the only frequency dependence be that of K where

$$K = \frac{K_0}{(1 + s\tau_O)} \tag{36}$$

and K_0 is the zero frequency value for the photoconductor response. Inserting equation (36) into the denominator of equation (23a) for system response yields

$$1 + A_L = 1 + V_S R_f \frac{S_D}{R_D} \frac{K_0}{(1 + s\tau_O)} \tag{37}$$

From standard feedback analysis (see ref. 9) it is known that the impulse response for this system is found by determining the roots of the function in equation (37). In this case there is only one root, that is,

$$s = -\frac{1}{\tau_o}\left(1 + V_s R_f \frac{S_D}{R_D} K_0\right) \tag{38}$$

Thus, there is a single root yielding a single response pole which, in turn, has associated with it the 3 dB frequency given by

$$f_{3dB} = \frac{1}{2\pi\tau_o}\left(1 + V_s R_f \frac{S_D}{R_D} K_0\right) \tag{39}$$

It is easy to see that as the loop gain increases, so does the effective 3 dB frequency.

First order analysis.- Unfortunately, this simple situation does not exist in practice. If the operational amplifier is properly modeled, it must include at least two time constants (ref. 8). The first time constant would be associated with a frequency at approximately the operational amplifier's unity gain frequency f_T multiplied by the factor R_λ/R_f. (As noted earlier, R_f is made larger than R_λ so that its noise contribution will be less than that of R_λ.) The second time constant is associated with a high frequency pole in the operational amplifier's response. The operational amplifier's response is assumed to have the following form:

$$A = \frac{R_f}{(1 + s\tau_1)(1 + s\tau_2)} \tag{40}$$

where $\tau_1 = \frac{R_\lambda}{R_f}\frac{1}{2\pi f_T}$, and $\tau_2 = \frac{1}{2\pi f_2}$ depends on the particular operational amplifier.

The operational amplifier response and the response of the photoconductor are considered to have the dominant effect on system performance, as has turned out in practice. It should be noted that a three-pole feedback system always becomes unstable. All of this modifies what was stated earlier for the ideal case: a simple increase in loop gain does not always increase frequency response. Not only instability can occur, but it matters which of the loop gain parameters V_s, R_f, S_D, or R_D is increased, and what value R_λ has.

For any value of loop gain there are three poles in the system. At low loop gain the poles are near their origins (corresponding to the open loop case). As the loop gain increases, one pole decreases in effect (and may be neglected) and the other two poles approach one another, eventually meeting. The latter two poles split to form conjugate frequency pairs, representing the onset of ringing or overshoot. As the gain is further increased, the two poles eventually acquire positive real parts and represent unbounded output for finite input, or instability.

Effect of parameters.- In order to demonstrate the effect of the various parameters in extending the frequency response, an assumption is made that the higher frequency operational amplifier pole has negligible influence. This assumption is found to be true in practice, especially in the useful range of loop gains which are those below the point of overshoot.

Under this assumption, the closed loop system poles can be expressed as the solutions of a quadratic, which are

$$s_{1,2} = \frac{\left(\tau_o + \frac{R_\lambda G_f}{2\pi f_T}\right) \pm \left[\left(\tau_o + \frac{R_\lambda G_f}{2\pi f_T}\right)^2 - \frac{4\tau_o R_\lambda G_f}{2\pi f_T}(1 + k)\right]^{1/2}}{\frac{2\tau_o R_\lambda G_f}{2\pi f_T}} \tag{41}$$

where $k = K_0 V_s R_f \frac{S_D}{R_D}$.

In general $\tau_o >> \frac{R_\lambda G_f}{2\pi f_T}$ and equation (41) can, with $\tau_1 = \frac{R_\lambda G_f}{2\pi f_T}$, be reduced to the expression

$$s_{1,2} = -\frac{1}{2\tau_1}\left\{1 \pm \left[1 - 4\frac{\tau_1}{\tau_o}(1 + k)\right]^{1/2}\right\} \tag{42}$$

The point of critical damping occurs when equation (42) has a real part and an imaginary part which are equal. This point is easily found to be

$$k = \frac{\tau_o}{2\tau_1} - 1 \tag{43}$$

Note that the greater frequency response is achieved for the smaller value of τ_1. The situation is more complicated if R_f is varied since it causes τ_1 to vary. It is beyond the scope of this analysis to pursue the effect of R_f variation except to note that increasing R_f yields a smaller value of critical damping loop gain. The best method for increasing bandwidth is to maximize the factor $K_0 \frac{S_D}{R_D} V_s$ while holding R_f constant.

Operating Range and Noise

The last analytical point to be discussed concerning the optical feedback is its dynamic range; that is, how many unity signal-to-noise ratio levels are within the bias offset of the optical feedback. It can easily be seen that the dynamic range concept is crucial because it is only by means of the bias offset that negative feedback can be realized. Once the input signal plus noise exceeds the bias level, then signal clipping must

occur. The situation is further aggravated by the fact that the bias light generates photon noise in the CdS, and wide frequency operation of the system must particularly take into account the decrease in dynamic range from this mechanism.

To give concreteness to these remarks, attention is directed to a case in which no excess noise is generated in the system and the photoconductor is assumed nearly photon noise limited. As a point of comparison, it is useful to introduce the noise in a photon stream with rate Φ, which from reference 7 is

$$\Phi_N^2 = 2\Phi\Delta f \tag{44}$$

or, when the energy per particle is included, the rms noise power in a photon stream at a frequency ν, which is

$$P_N = h\nu(2\Phi\Delta f)^{1/2} = (2h\nu P\Delta f)^{1/2} \tag{45}$$

When evaluated at a wavelength of 6500 Å, ΔB of 1 Hz, and a power of 10^{-6} W, this equation yields

$$P_N(6500\ \text{Å}) = 6.3 \times 10^{-13}\ \text{W}/\text{Hz}^{1/2} \tag{46}$$

Note that there is a point at each power level at which, for a certain bandwidth ΔB, the rms noise is equal to the power P which has given rise to it.

To see how the point of equivalence of rms noise and incident power can affect the dynamic range of the optical feedback with CdS (as it must, since CdS is, or is nearly, photon noise limited), use must be made of equations (23) in the form

$$V_o = -\frac{R_D}{S_D}\alpha P_i - \frac{R_D}{S_D}P_e + \frac{R_D}{S_D} \tag{47}$$

where

$$P_N = \frac{1}{V_s K_0}\left(\frac{4eGV_s}{R_\lambda}\right)^{1/2}(\Delta f)^{1/2}$$

that is, it has been assumed that the only noise being generated is from the CdS and is the g-r noise component of equation (13) referred back as an equivalent radiant noise power through equation (22). Further the frequency dependences have been assumed to cancel. In the condition of zero input radiant power ($P_i = 0$), the CdS conductivity is generated only by the bias radiant energy P_e, so that

$$G_\lambda = \frac{1}{R_\lambda} = K_0 P_e \tag{48}$$

The dynamic range ρ is defined as the number of rms noise levels in the offset or bias and can be developed as follows:

$$\rho = \frac{P_e}{P_N} = \frac{K_0 V_s P_e}{(4eGV_s K_0 P_e)^{1/2}(\Delta f)^{1/2}} \tag{49}$$

This equation can be reduced to

$$\rho = \frac{(K_0 V_s P_e)^{1/2}}{(4eG)^{1/2}(\Delta f)^{1/2}} \tag{50}$$

Using typical values for CdS-type materials and applications (that is, $K = 10^3$, $V_s = 10$ V, $G = 10^4$, $\Delta B = 10^4$, and $e = 1.6 \times 10^{-19}$ C) gives

$$\rho = 0.125(P_e)^{1/2} \times 10^8 \tag{51}$$

Note that since the operation of the optical feedback is to maintain the sum $P_e + P_i$ constant, then the noise is constant with input signal. Thus, the minimum detectable signal is set by the noise in P_e.

Table I lists P_e, P_N, and ρ values so that it is possible to compare the minimum detectable signal with the dynamic range at a particular bias light level. For comparison, equation (45) can be solved for the 6500 Å radiant energy value at which it and its rms value in 10 kHz are the same, so that ρ is unity. Thus,

$$P_N^2 = P^2 = 2h\nu P \times 10^4 \tag{52a}$$

$$P = 6.4 \times 10^{-15} \tag{52b}$$

which confirms the analytical results in the table, at least for the assumptions and approximations made here.

It may be said that the primary limitation on operation of photon noise limited photoconductors, such as CdS, with optical feedback in any low light level application may be the dynamic range rather than the frequency response. Careful note should be taken of the fact that frequency response and dynamic range are somewhat interrelated.

APPLICATION TO CADMIUM SULFIDE

Preliminary Considerations

In order to illustrate the foregoing analysis of optical feedback and discussion of CdS-type photoconductors, this section describes the implementation of an optical feedback and CdS system. Basic configurations that bear on attaining the greatest bandwidth and greatest signal-to-noise ratio are presented. An experimental system is also described along with results which verify the analysis presented earlier.

Cadmium sulfide has been chosen for study because it has a detectivity higher than that of any other photoconductor and is the only one that can reach the high detectivities of photomultipliers. Reference 4 gives a peak detectivity D^* of 3.5×10^{14} for CdS and for comparison the same reference gives a peak detectivity of 5×10^{14} for the 1P21 photomultiplier. The spectral sensitivity of CdS covers the visible wavelength range 4000 Å to 7000 Å.

The CdS photocell employed was a typical device whose sensitive area is the serpentine structure shown in figure 3(a). As will become evident, the choice of the particular CdS detector configuration is not critical and system performance depends primarily on basic material sensitivity. For this reason attention is focused on a typical group of medium sensitivity photocells, the Clairex CL-600 series, which were selected because of their availability.

Shown in figures 3(b) and 3(c) are manufacturer's data on the spectral response and on the resistance as a function of illumination of the type 5 CdS material available in the CL-600 series of cells. Listed in table II is the response time of the type 5 CdS materials available in the CL-600 series at various light levels.

The type 5 material has the longest 1000 lm/m^2 time constant, which, according to reference 3, is approximately the electron lifetime. This, along with low resistivity, implies a high sensitivity and high gain photoconductor.

A test was made of the sensitivity of the type 5 material at various incident power levels and the results are listed in table III. Note that although the sensitivity is not as high as the highest attainable, it is at least of the same order of magnitude.

To arrive at an idea of the effective noise power, dynamic range, and frequency response that correspond to a particular cell resistance, let it be assumed that the CdS cell is masked off to an active area of approximately 0.02 cm by 0.10 cm. This reduces the length of the serpentine active region by a factor of 25 and hence increases the resistance of the photoconductor at each particular illumination point by this same factor.

If a V_S of 10 V is assumed and typical values for the type 5 material are chosen $\mu = 200\ cm^2/V\text{-}sec$ and $\tau = 10^{-2}$ sec, then the gain G is, from equation (9),

$$G = \frac{\mu\tau}{l^2} V_S = 5.0 \times 10^4 \tag{53}$$

The noise current is then determined from equation (13) to be, neglecting 1/f noise,

$$I_{N,t} = 5.6 \times 10^{-7} \left(\frac{1}{R_\lambda}\right)^{1/2} \tag{54}$$

With a value for the peak sensitivity of $0.5\ S\text{-}cm^2/W$ and an electrode separation of 0.02 cm, the noise equivalent power per $Hz^{1/2}$ is

$$P_N = 4 \times 10^{-11} (R_\lambda)^{-1/2} \tag{55}$$

Knowing R_λ also allows the approximate determination of τ_O, the CdS internal response time, through the use of the data in figure 3(c) and table II. If the system loop gain is also known, the frequency response at particular bias levels can be predicted from the loop gain measurement, the value of τ_O from table II, and equation (23a) or (39).

Experimental Results

The CL605 photoconductor was incorporated into a circuit whose schematic is shown in figure 4. The CdS was masked down to the approximate dimensions described previously (0.02 cm by 0.10 cm) and the value of the LED series resistance R_D was varied to change the loop gain. The bias supply V_B was also made variable so as to permit control of the bias light power $P_e \left(= \frac{1}{K_O V_S} \frac{V_B}{R_B}\right)$.

The maximum value of K_O $(= S/l^2)$ is then $0.5 \times 2500 \approx 10^3$ S/W at 5500 Å while the LED radiates at 6600 Å with an output power of 3 mW/A. Combining this value for K_O with the CdS response at 6600 Å of 70 percent of peak gives a value for K_O of 7×10^2 S/W. The supply voltage V_S was set at 22.5 V and R_f at 10 MΩ. The value of S_D had to be determined by measurement, whereas the value of R_D was allowed to vary as a means of adjusting loop gain. (The loop gain was maintained at a particular value by setting R_D while S_D, R_f, and V_S were held constant throughout.) Then, the operating point (bias light) was varied by adjusting V_B over a range of 15 V down to a minimum level for operation. At each value of V_B, the loop gain was measured by using equation (16) which yields a value for G_λ. The loop gain can be found from these

measurements and the fact that (see ref. 9) the change in the photoconductor current ΔI at the operational amplifier input for a change in V_B is

$$\Delta I = V_S\left(\frac{1}{R_{\lambda,1}} - \frac{1}{R_{\lambda,2}}\right) = V_S \frac{K_0 S_D}{R_D} V_o = A_L \frac{V_o}{R_f} \tag{56}$$

where $R_{\lambda,1}$ and $R_{\lambda,2}$ are values of photoconductor resistance at two measured bias voltages.

The results are plotted in figure 5 for values of R_D = 430 Ω, 5.1 kΩ, 9.8 kΩ, and 47 kΩ. Extensive data were taken for the 430 Ω and 5.1 kΩ cases, whereas data were taken for the 9.8 kΩ and 47 kΩ cases primarily to indicate trends. Notice should be given to the gradual decrease in loop gain as a function of operating point as expressed by the LED static current. Since the change is of the same form for each value of loop gain parameter R_D, this indicates a nonlinear change in either the LED current (through S_D) or CdS (through K_0 or S). Manufacturer's data for the LED indicate linear operation so that the nonlinearity must be ascribed to the CdS.

Frequency response measurements showed no indication of peaking; this result is in agreement with the earlier analysis on system stability. The frequency response curves had 3 dB frequencies which are shown in figure 6 plotted against operating point as expressed by the LED static current.

To illustrate the idea of increased frequency response with an increase in loop gain (the "gain bandwidth" trade-off), a summary of predicted frequency response and measured frequency response is given in table IV for V_B = 15 V. The bias light on R_λ yielded a value of resistance equal to approximately 1 MΩ. By referring to manufacturer's data on the device and taking into account the masking of the detector, the bias illumination was determined to be 7.0 lm/m^2. Extrapolating from table II gives an internal 3 dB frequency of approximately 0.8 Hz. If the gain bandwidth idea applies, then the loop gain times the internal CdS 3 dB frequency should be the system frequency. In particular at R_D = 430 Ω, the loop gain was found to be 9820. Multiplying this value with the internal CdS 3 dB frequency of 0.8 Hz gives a predicted value of 7856 Hz compared with a measured value of 4500 Hz. Also included in table IV is a comparison of various predicted 3 dB frequencies derived from the loop gains just above it in value under the assumption that the loop gain varies as the ratio of any two diode series resistances. The 3 dB frequency at R_D = 430 Ω is used as a starting reference. Given the uncertainties in actual masking of the CdS (which affects the resistance for a given illumination) and in typical manufacturing tolerances, there is good agreement of the predicted and measured 3 dB frequencies.

Noise spectra were measured at the approximate operating point mentioned previously. The noise spectrum results for the different loop gains are shown in figure 7. There is clear evidence that in the commerical CdS cells used here, there was significant 1/f noise. This is most evident in the 430 Ω case. If the 1/f noise is assumed to be dominant in the commercial cells, then the noise spectra corresponding to the lower values of loop gain can be explained as follows: As long as the loop gain is greater than 1, its reciprocal has a 6 dB per octave increase with frequency. The 1/f noise has a 3 dB per octave decrease with frequency (since 1/f noise voltage varies as $(1/f)^{1/2}$). The product of these two shows a 3 dB per octave overall increase with frequency. As soon as the loop gain approaches unity, it thereafter remains at this value, while the 1/f noise continues to cause an overall 3 dB per octave decrease in noise with frequency. Note that the point of transition should be the point at which the loop gain approaches unity and should represent the system 3 dB response frequency.

Identified on the noise spectra curves are the measured 3 dB frequencies at this operating point. They coincide reasonably well with the transition from 3 dB per octave rise to 3 dB per octave fall in the noise. Attention should also be drawn to the fact that all the noise spectra coincide at points in the noise spectra sufficiently above the individual 3 dB frequencies.

The degree to which the 1/f noise exceeds the g-r noise can be found by calculating the value for the g-r noise current from equation (55) to be (at $R_\lambda \approx 1 \times 10^6$ Ω) $I_{N,t} = 5.6 \times 10^{-10}$ A/Hz$^{1/2}$. Using the highest loop gain of 10^4 for the 430 Ω resistor and $R_f = 10$ MΩ allows the use of the g-r noise component of equation (30) to yield the output noise voltage

$$V_{N,S} \approx \frac{R_D}{S_D V_S K_0}\left(\frac{4eV_S G}{R_\lambda}\right)^{1/2}(\Delta f)^{1/2} = 0.56 \times 10^{-6}\ \text{V/Hz}^{1/2} \qquad (57)$$

Thus, at 1 Hz the measured 1/f noise in figure 7 is about three to four times the predicted g-r noise value. This is not surprising since the CL605L photocell is a commercial device and is not intended to yield the lowest noise possible for CdS. Nevertheless, it should be noted that even with the 1/f noise, the output noise level is only about an order of magnitude higher than the photon-noiselike g-r noise throughout the 10 kHz frequency range shown in figure 7.

Since the noise is primarily 1/f-like for this case, measurement of dynamic range would not be useful in predicting the dynamic range for the situation in which the g-r noise dominates. However, a rough calculation can be made by inspection of figure 7. Using the 3 dB frequencies as the bandwidth and the low frequency noise values yields an

idea of total rms noise in that bandwidth. The dynamic range is then given by dividing the rms noise into the bias voltage. The resulting values for the various resistances are

ρ = 2104:1 for 47 kΩ

ρ = 797:1 for 9.8 kΩ

ρ = 440:1 for 5.1 kΩ

ρ = 139:1 for 430 Ω

As expected the dynamic range decreases at constant operating point and increased loop gain. This should be compared with data in table I, in which only g-r noise was assumed. The value for P_e can be obtained by using the relation $P_e = \frac{1}{K_0 R_\lambda}$ which in this case yields $P_e \approx \frac{10^{-6}}{10^3} = 10^{-9}$ W. The loss of dynamic range ρ would be further aggravated if the biasing were decreased (yielding a longer internal CdS response time) and the loop gain were increased (to regain lost bandwidth).

Even though, as was noted earlier and demonstrated here, the dynamic range loss seems to be the limiting factor in the low light level operation of CdS with optical feedback, there are redeeming factors to be considered.

As was discussed earlier, the optical feedback maintains, or attempts to maintain, the summed input and feedback light constant on the CdS. This maintenance of operating point is useful since simple frequency compensation of CdS is impractical because its internal 3 dB frequency is ambient illumination dependent. The optical feedback stabilizes the operating point, and hence the effective response time of the CdS, which permits simple frequency compensation.

Stated another way, requirements of a certain dynamic range and minimum detectable signal per $Hz^{1/2}$ may well limit the available 3 dB frequency obtainable. However, the principle of stable operating point allows simple frequency reconstitution to be performed outside the optical feedback system in a regime of very much larger available dynamic range.

CONCLUDING REMARKS

Analysis and experimental results have confirmed the capability of optical feedback to extend the frequency response of cadmium sulfide and render it useful at frequencies which are orders of magnitude above the photoconductor's internal 3 dB frequency. Furthermore, for suitable operating bias, the optical feedback technique need not degrade

the available signal-to-noise ratio. This result is important because cadmium sulfide is nearly a photon noise limited solid state photodetector, making it almost unique in that respect. However, the optical feedback is not without its limitations. The most important difficulty does not arise from stability considerations which limit the bandwidth extension available. Rather, the primary limitation arises from the interaction of bandwith, noise, and the required operating bias. For a fixed bandwidth as the bias light is decreased, it has been shown that, the noise generated by the light bias will eventually exceed, in rms value, the value of the light bias. This loss of dynamic range results in clipping and system saturation.

However, the effect that the optical feedback has in stabilizing the photoconductor operating point can be turned to advantage to circumvent the possible loss in dynamic range. Since the internal response time of CdS depends on its operating point, it is possible that this can be accomplished through optical feedback with conventional frequency reconstitution. The full photosensitivity and bandwidth are then still available, but only as a result of the optical feedback.

Even though the dynamic range loss seems to be the limiting factor in the low light level operation of CdS with optical feedback, there are redeeming factors to be considered. The optical feedback maintains, or attempts to maintain, the summed input and feedback light constant on the CdS. This is in itself extremely useful for the following reason: Simple frequency compensation of CdS is impractical because its internal 3 dB frequency is ambient illumination dependent. The optical feedback stabilizes the operating point, and hence the effective response time of the CdS, and so permits simple frequency compensation. Stated another way, requirements of a certain dynamic range and minimum detectable signal per $Hz^{1/2}$ may well limit the 3 dB frequency obtainable. However, the principle of stable operating point allows simple frequency reconstitution to be performed outside the optical feedback system over a very much larger available dynamic range.

Langley Research Center,
National Aeronautics and Space Administration,
Hampton, Va., July 30, 1974.

REFERENCES

1. Van Vliet, K. M.: Noise in Semiconductors and Photoconductors. Proc. IRE, vol. 46, no. 6, June 1958, pp. 1004-1018.

2. Katzberg, Stephen J. : An Investigation of Optical Feedback To Extend the Frequency Response of Solid-State Detector Systems. NASA TM X-2676, 1972.

3. Bube, Richard H.: Photoconductors. Photoelectronic Materials and Devices, Simon Larach, ed., D. van Nostrand Co., Inc., c.1965, pp. 100-139.

4. Kruse, Paul W.; McGlauchlin, Laurence D.; and McQuistan, Richmond B.: Elements of Infrared Technology. John Wiley & Sons, Inc., 1963.

5. Monteith, L. K.; Littlejohn, M. A.; and Hauser, J. R.: An Evaluation of Solid State Phenomena and Devices for Sensor Applications. NASA CR-111873, 1971.

6. Humphrey, James N.: Optimum Utilization of Lead Sulfide Infrared Detectors Under Diverse Operating Conditions. Appl. Opt., vol. 4, no. 6, June 1965, pp. 665-676.

7. Rose, A.: Noise Currents. Photoelectronic Materials and Devices, Simon Larach, ed., D. van Nostrand Co., Inc., c.1965, pp. 222-238.

8. Graeme, Jerald G.; Tobey, Gene E.; and Huelsman, Lawrence P., eds.: Operational Amplifiers – Design and Applications. McGraw-Hill Book Co., Inc., c.1971.

9. Brown, Robert Grover; and Nilsson, James William: Introduction to Linear Systems Analysis. John Willey & Sons, Inc., c.1962.

TABLE I.- DYNAMIC RANGE AND MINIMUM DETECTABLE SIGNAL

P_e, watts	P_N, watts, for –		ρ for –	
	10^4 Hz	10^2 Hz	10^4 Hz	10^2 Hz
1	0.8×10^{-7}	0.8×10^{-8}	1.25×10^{7}	1.25×10^{8}
10^{-2}	$.8 \times 10^{-8}$	$.8 \times 10^{-9}$	1.25×10^{6}	1.25×10^{7}
10^{-4}	$.8 \times 10^{-9}$	$.8 \times 10^{-10}$	1.25×10^{5}	1.25×10^{6}
10^{-6}	$.8 \times 10^{-10}$	$.8 \times 10^{-11}$	1.25×10^{4}	1.25×10^{5}
10^{-8}	$.8 \times 10^{-11}$	$.8 \times 10^{-12}$	1.25×10^{3}	1.25×10^{4}
10^{-10}	$.8 \times 10^{-12}$	$.8 \times 10^{-13}$	1.25×10^{2}	1.25×10^{3}
10^{-12}	$.8 \times 10^{-13}$	$.8 \times 10^{-14}$	1.25×10	1.25×10^{2}
10^{-14}	$.8 \times 10^{-14}$	$.8 \times 10^{-15}$	1.25	1.25×10
10^{-16}	$.8 \times 10^{-15}$	$.8 \times 10^{-16}$	.125	1.25

TABLE II. - CHARACTERISTICS OF CdS RESPONSE TIME AS A FUNCTION OF ILLUMINATION

[From manufacturer's data]

Illumination,[1] lumens/meter^2	0.1	1.0	10	100	1000
Rise time, seconds	5.80	0.82	0.140	0.035	0.010
Decay time, seconds	2.96	0.56	0.110	0.043	0.014

[1]Manufacturer's data were in footcandles.

TABLE III.- SENSITIVITY OF CdS CELL

AS A FUNCTION OF ILLUMINATION

Incident power, W	R_λ, kΩ	S at 5895 Å, S-cm^2/W	S at peak wavelength, S-cm^2/W
1.125×10^{-7}	21	0.12	0.17
.900	22.7	.28	.40
.675	28.6	.256	.37
.563	32.4	.348	.50
.450	39.5	.256	.37
.338	48	.28	.40
.225	63.4	.32	.46
.113	99	.28	.40

TABLE IV.- CALCULATED AND MEASURED 3 dB FREQUENCIES

[3 dB frequency at R_D = 430 Ω used as reference]

Calculated 3 dB frequency, Hz, at –				Measured 3 dB frequency, Hz
430 Ω	5.1 kΩ	9.8 kΩ	47 kΩ	
4500	---	---	---	4500
350	---	---	---	380
197	182	---	---	200
41	38	42	---	48

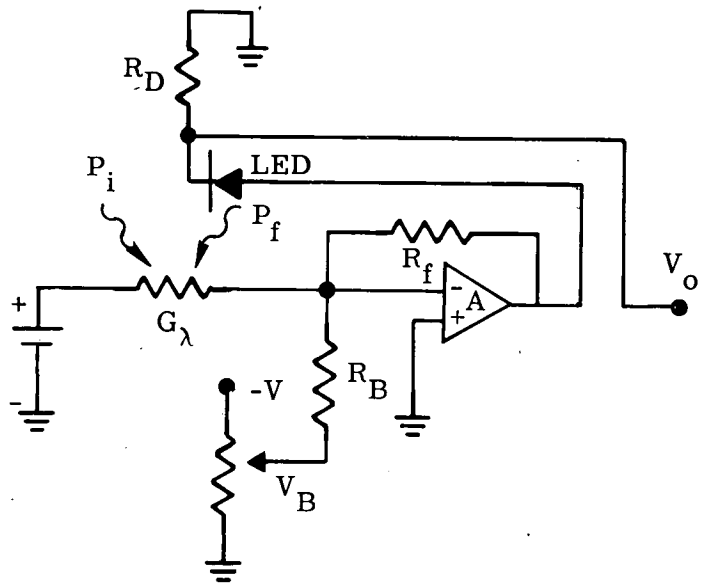

Figure 1.- Optical feedback concept.

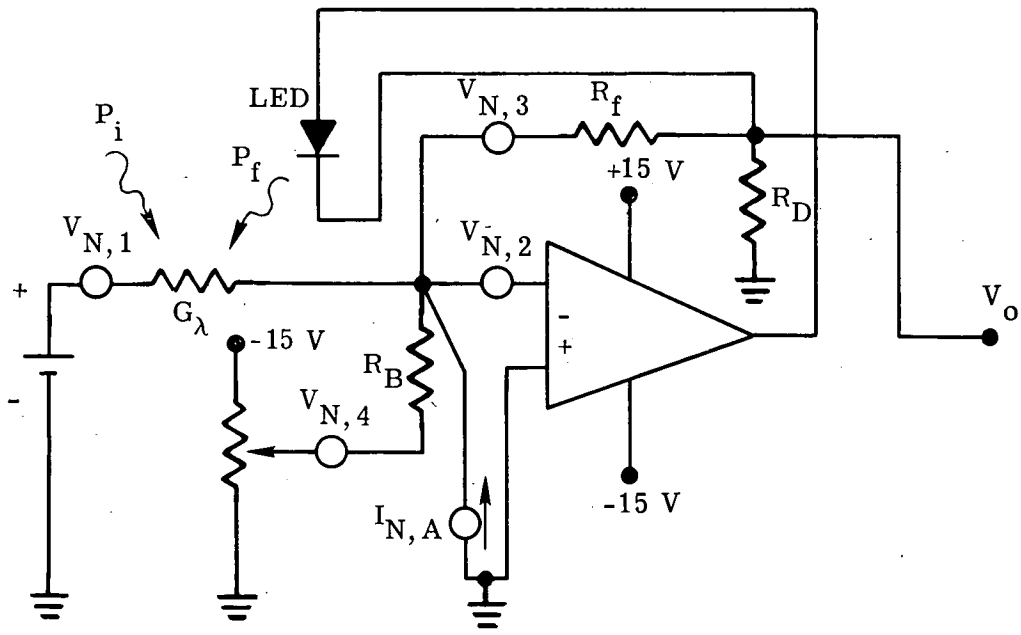

Figure 2.- Optical feedback circuit with noise sources.

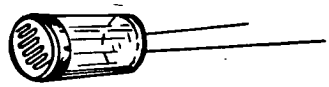

(a) Layout.

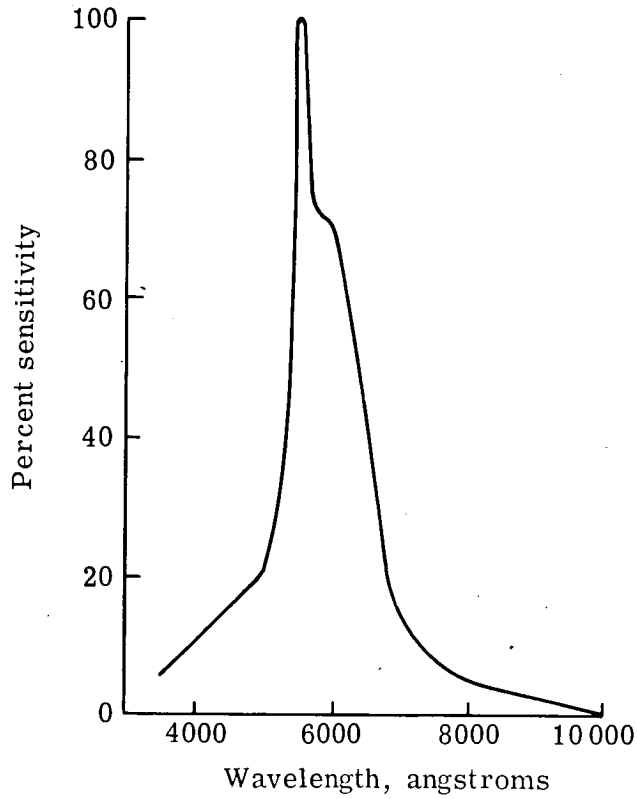

(b) Spectral sensitivity.

Figure 3.- Characteristics of Clairex photocell. (From manufacturer's data sheets.)

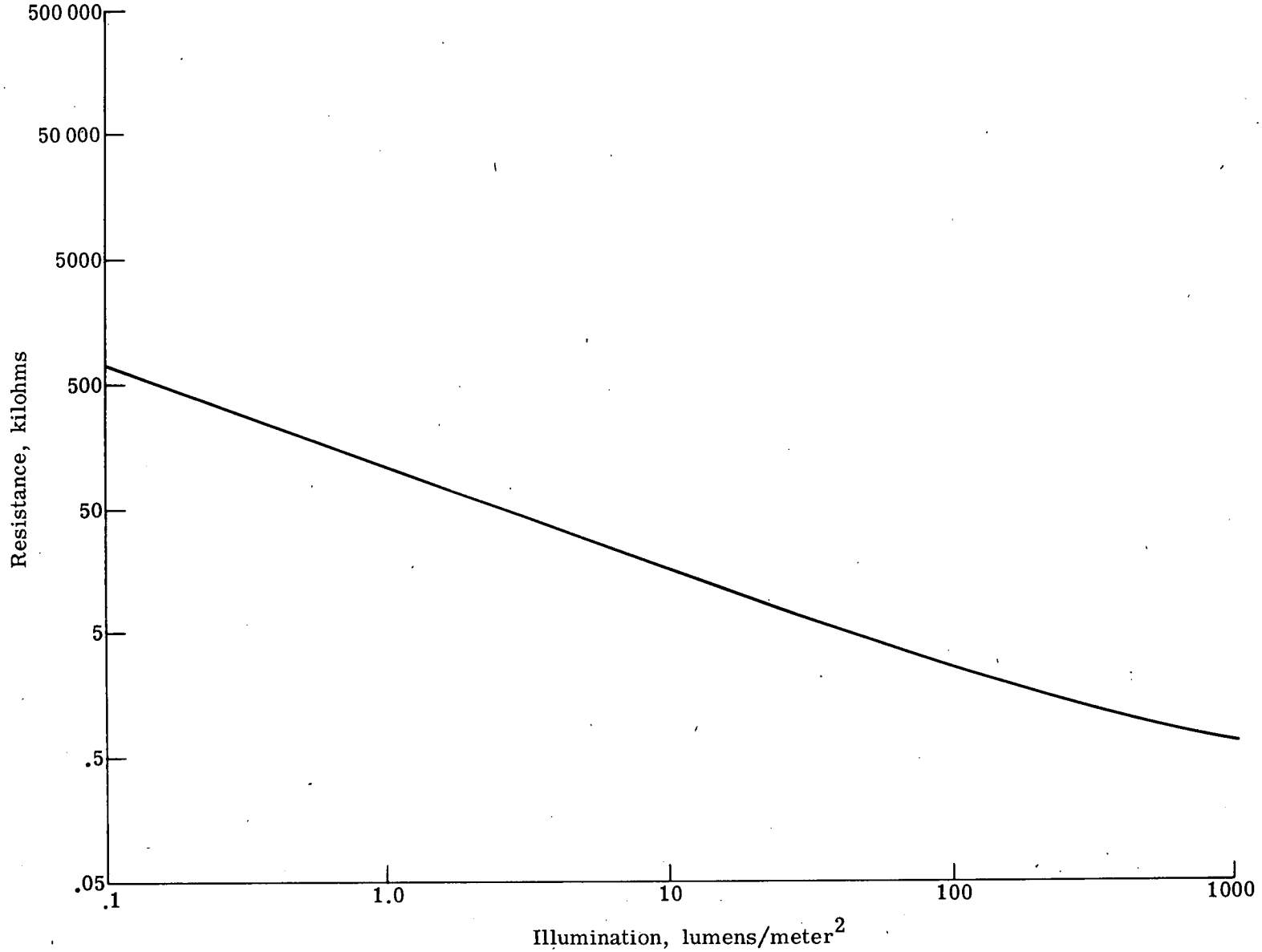

(c) Resistance as a function of illumination for CdS cell.

Figure 3.- Concluded.

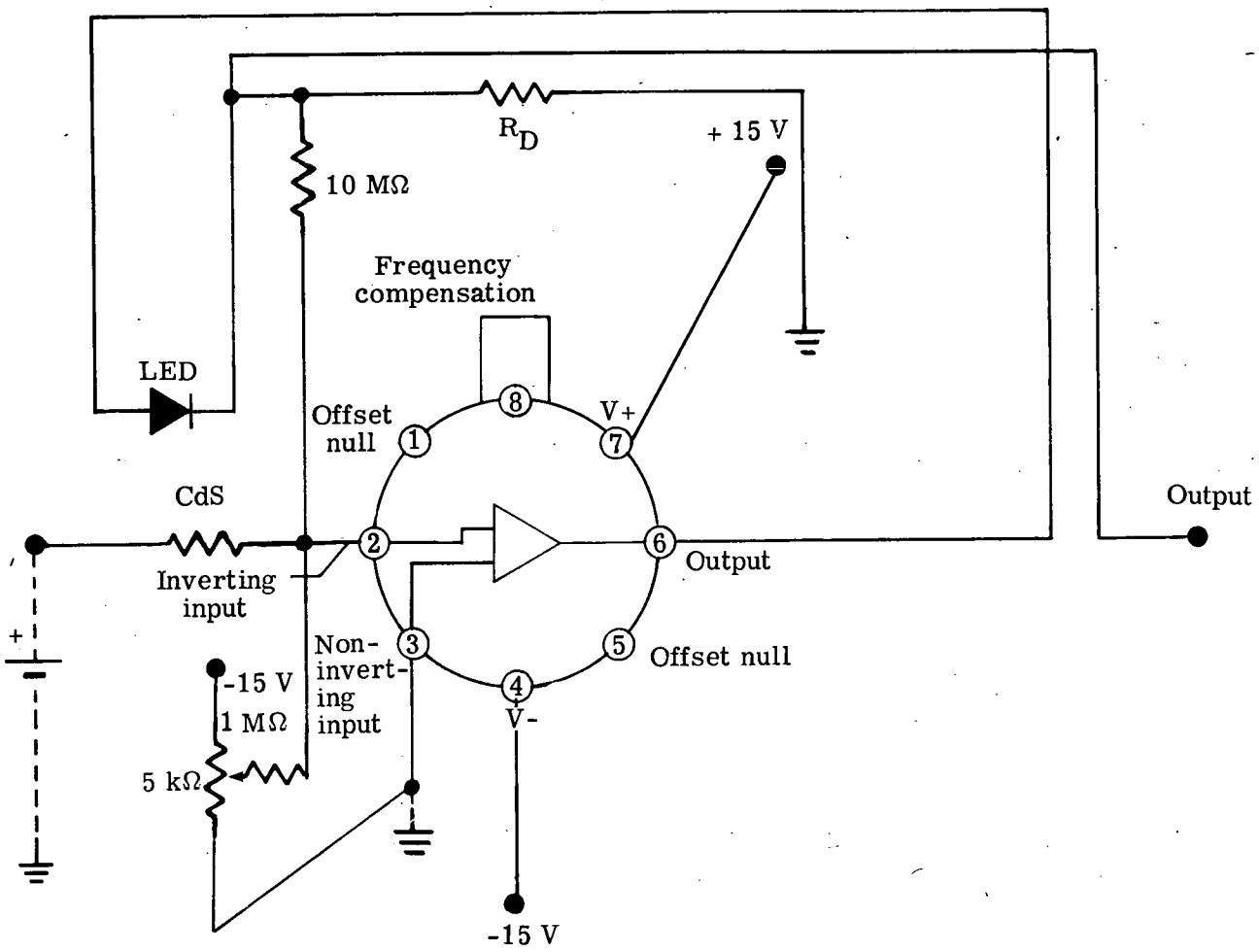

Figure 4.- Schematic diagram of optical feedback circuit.

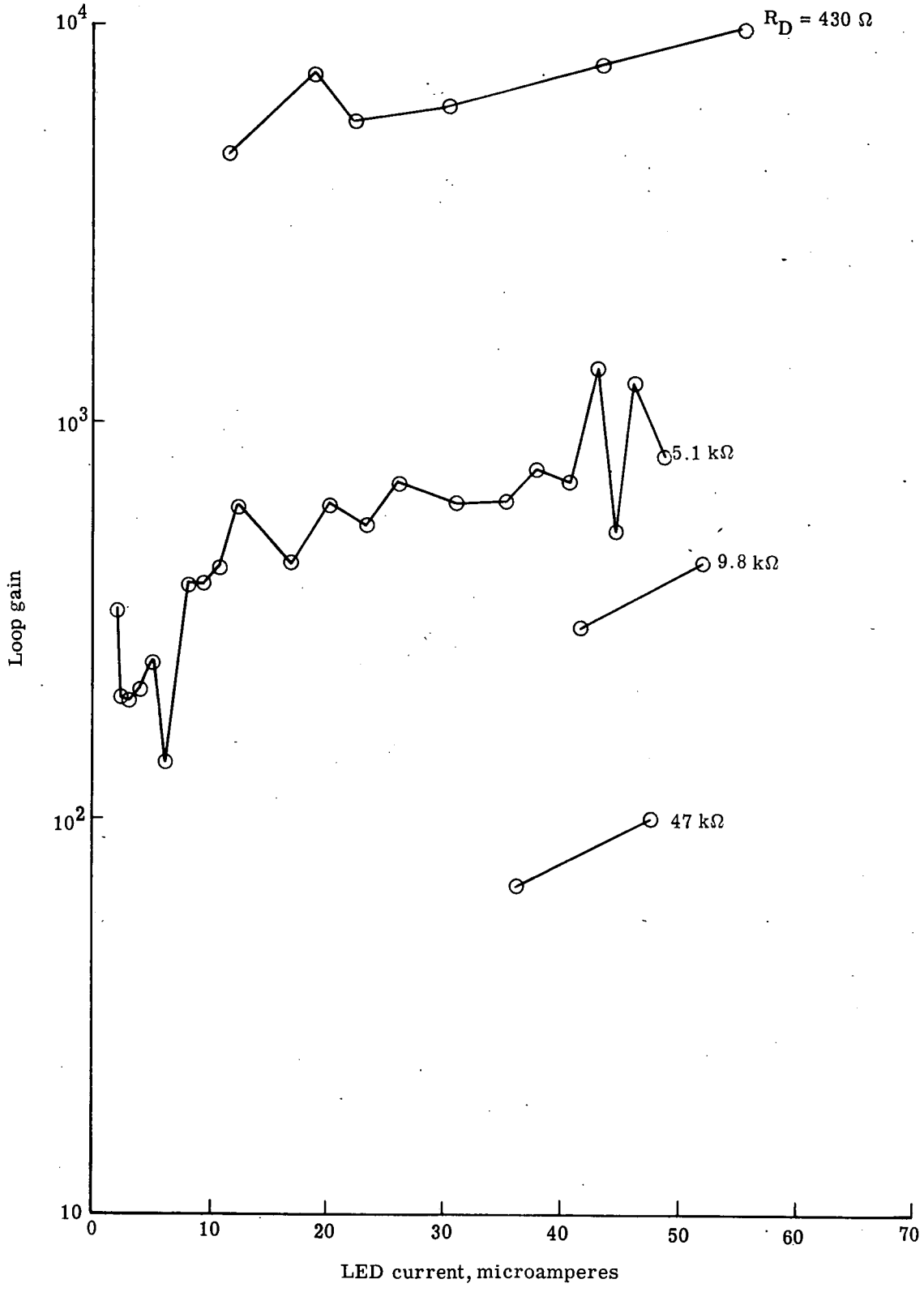

Figure 5.- Variation of loop gain with operating point at various LED resistances.

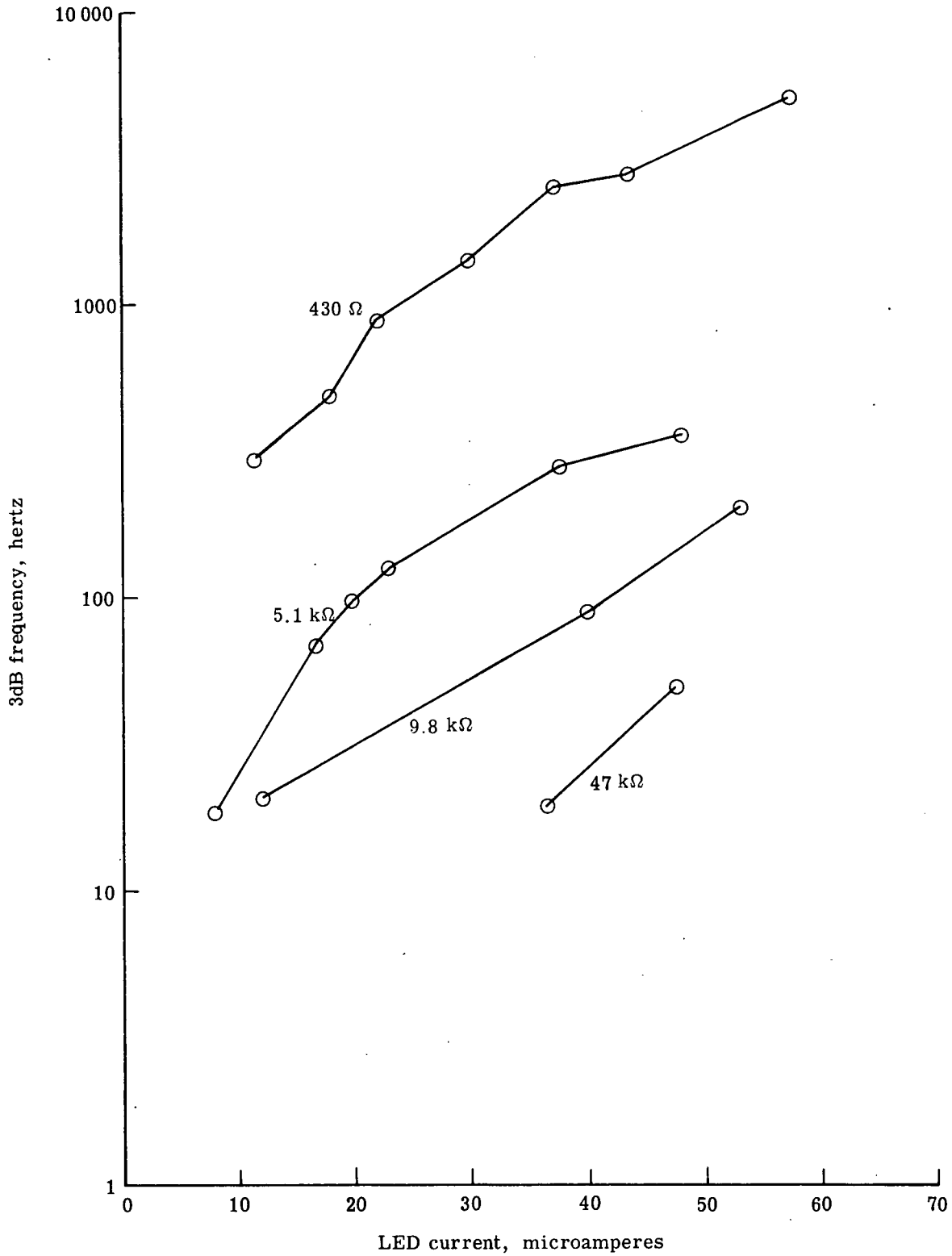

Figure 6.- Variation of system 3 dB frequency with operating point at various LED resistances.

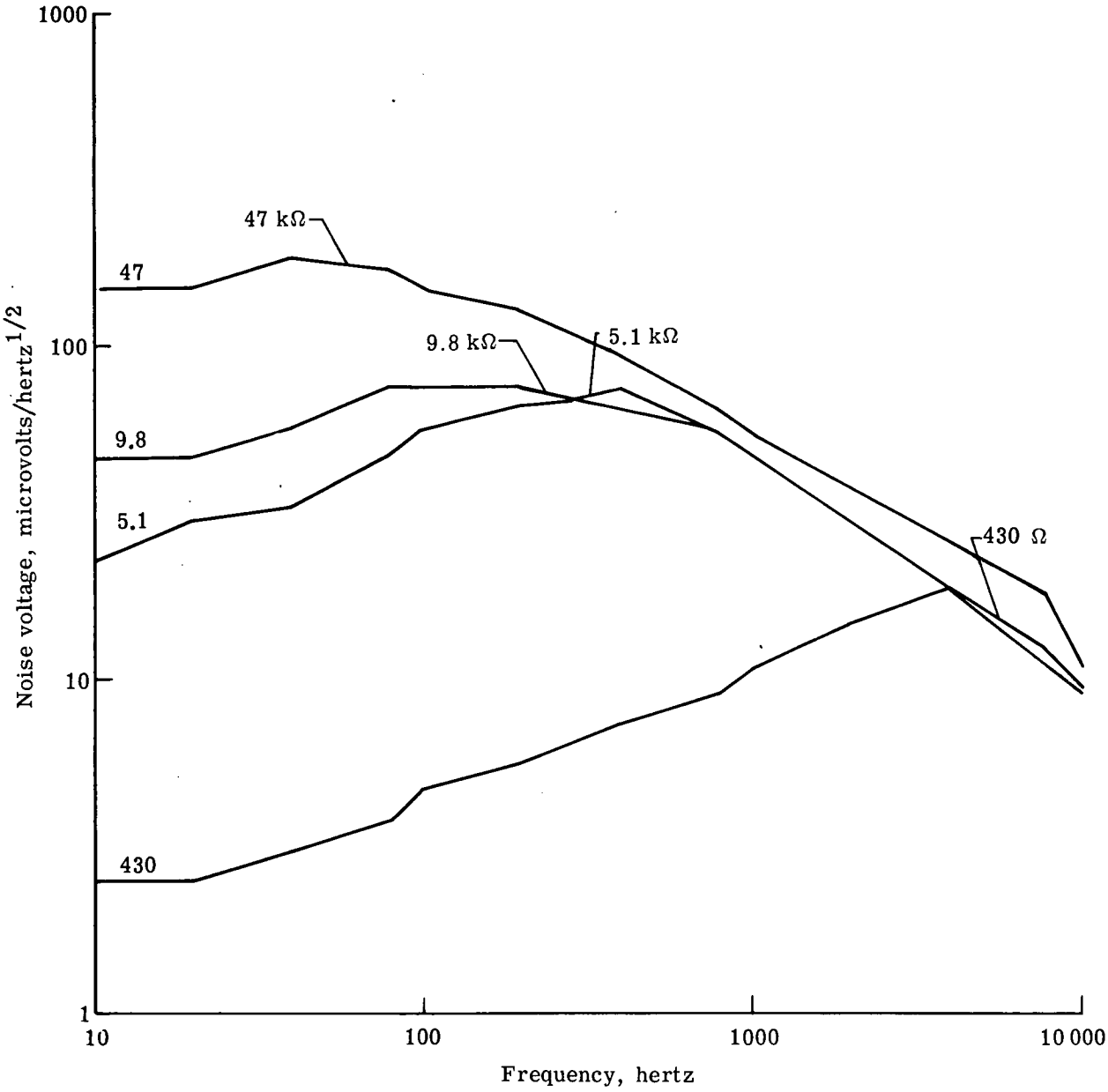

Figure 7.- Noise spectra with various LED series resistances. (Leaders indicate 3 dB frequencies associated with each LED resistance.)

NATIONAL AERONAUTICS AND SPACE ADMINISTRATION
WASHINGTON, D.C. 20546

OFFICIAL BUSINESS
PENALTY FOR PRIVATE USE $300

SPECIAL FOURTH-CLASS RATE BOOK

POSTAGE AND FEES PAID
NATIONAL AERONAUTICS AND SPACE ADMINISTRATION
451

U.S.MAIL

POSTMASTER: If Undeliverable (Section 158 Postal Manual) Do Not Return

"The aeronautical and space activities of the United States shall be conducted so as to contribute . . . to the expansion of human knowledge of phenomena in the atmosphere and space. The Administration shall provide for the widest practicable and appropriate dissemination of information concerning its activities and the results thereof."

—NATIONAL AERONAUTICS AND SPACE ACT OF 1958

NASA SCIENTIFIC AND TECHNICAL PUBLICATIONS

TECHNICAL REPORTS: Scientific and technical information considered important, complete, and a lasting contribution to existing knowledge.

TECHNICAL NOTES: Information less broad in scope but nevertheless of importance as a contribution to existing knowledge.

TECHNICAL MEMORANDUMS: Information receiving limited distribution because of preliminary data, security classification, or other reasons. Also includes conference proceedings with either limited or unlimited distribution.

CONTRACTOR REPORTS: Scientific and technical information generated under a NASA contract or grant and considered an important contribution to existing knowledge.

TECHNICAL TRANSLATIONS: Information published in a foreign language considered to merit NASA distribution in English.

SPECIAL PUBLICATIONS: Information derived from or of value to NASA activities. Publications include final reports of major projects, monographs, data compilations, handbooks, sourcebooks, and special bibliographies.

TECHNOLOGY UTILIZATION PUBLICATIONS: Information on technology used by NASA that may be of particular interest in commercial and other non-aerospace applications. Publications include Tech Briefs, Technology Utilization Reports and Technology Surveys.

Details on the availability of these publications may be obtained from:

SCIENTIFIC AND TECHNICAL INFORMATION OFFICE

NATIONAL AERONAUTICS AND SPACE ADMINISTRATION

Washington, D.C. 20546